

Characterization of a NIR absorbing thienyl curcumin contrast agent for photoacoustic imaging

Electronic Supporting Information

Stephanie Bellinger,^a Maryam Hatami,^b Raymond E. Borg,^a Jeffrey La,^b Peter Catsoulis,^a Farha Mithila,^a Chandra Yelleswarapu,^{b*} Jonathan Rochford.^{a*}

Materials Spectroscopic grade acetonitrile and 5-dimethylamino-thiophene-2-carbaldehyde were purchased from Sigma Aldrich and used as received. ACS reagent grade toluene, dichloromethane and hexane for synthesis were purchased from Pharmco Aaper. Acetylacetonone difluoroboron (acacBF₂), **1** and **2** were prepared by previously reported methods and analytical data matched those of the literature.[1-3] **3** was obtained through the same modified Knoevenagel condensation by refluxing acacBF₂ with 5-dimethylamino-thiophene-2-carbaldehyde in toluene under an argon atmosphere. The product was sparingly soluble in toluene and yielded substantial precipitate upon cooling the reaction mixture. Analytically pure compound was obtained following a wash with cold toluene and recrystallization from dichloromethane:hexane (1:10). ¹H NMR (*d*-CDCl₃) δ ppm 3.10 (s, 12 H), 5.63 (s, 1H), 5.88 (d, 2H, *J* = 20 Hz), 5.89 (d, 2H, *J* = 4 Hz), 7.15 (d, 2H, *J* = 4 Hz), 7.93 (d, 2H, *J* = 20 Hz). HRMS (ESI-) calcd. for C₁₉H₂₁BF₂N₂O₂S₂ 422.1106, found 422.1112.

Physical Measurements ¹H-NMR spectra were recorded on an Agilent 400MHz spectrometer in *d*-chloroform (Aldrich) and the residual solvent signal ($\delta = 7.26$ ppm) was used as an internal reference point for reporting the chemical shift (δ).[4] Mass spectroscopy was carried out on a Q-ToF Premier using Negative ESI in V-mode. Cyclic voltammetry experiments were carried out on a CH Instruments 620E potentiostat. A standard three electrode cell was used under an atmosphere of argon with 0.1 M Bu₄NPF₆ in spectrophotometric grade acetonitrile as the supporting electrolyte. Glassy carbon (3-mm diameter) and Pt wire were used as working and counter electrodes respectively. A non-aqueous reference electrode was

used to minimize IR drop at the solvent interface. This consisted of a Ag wire in the same supporting electrolyte separated by a vycor frit. All cyclic voltammetry experiments were calibrated using ferrocene (Fc) as an internal pseudo reference due to the relative instability of the reference electrode employed and all redox potentials are thus reported in reference to the $\text{Fc}^{+/0}$ couple. As the redox couple equilibrium potential (E) could not be calculated due to irreversible behaviour, only cathodic (E_{pc}) or anodic (E_{pa}) peaks are reported for reduction and oxidation events, respectively. UV-Vis-NIR absorption spectra were recorded on an Agilent 8456 diode array spectrophotometer in spectrophotometric grade acetonitrile. Steady state and time-resolved fluorescence measurements were carried out on a Photon Technology International Quantamaster 40 & 25 fluorimeter at room temperature. Quantum yields were calculated by the optically dilute technique with fluorescein (aqueous NaOH, pH = 1, $\lambda_{\text{exc}} = 390$ nm, $\Phi_{\text{ref}} = 0.925$) and rhodamine 6G (neat acetonitrile, $\lambda_{\text{exc}} = 480$ nm, $\Phi_{\text{ref}} = 0.94$) used as reference standards according to Eq. 1.

$$\Phi_{\text{fl}} = (A_{\text{ref}}/A_{\text{s}})(I_{\text{s}}/I_{\text{ref}})(\eta_{\text{s}}/\eta_{\text{ref}})^2\Phi^{\text{ref}} \quad (1)$$

The subscript “s” refers to the unknown sample and the subscript “ref” to the reference sample, A is the absorbance at the excitation wavelength, I is the integrated emission area, and η is the solvent refractive index. Excitation and emission slits were both set to 5 nm. Fluorescence lifetimes (τ) were recorded at room temperature at the emission maximum following LED excitation at 456 nm or 572 nm. The radiative rate constant (k_{r}) and nonradiative rate constant (k_{nr}) were both calculated from ${}^1\tau$ and Φ_{fl} by using Eqs. 2-5.

$${}^1\tau = 1 / (k_{\text{r}} + k_{\text{nr}}) \quad (2)$$

$$\Phi_{\text{fl}} = k_{\text{r}} / (k_{\text{r}} + k_{\text{nr}}) \quad (3)$$

$$k_{\text{r}} = \Phi_{\text{fl}} / {}^1\tau \quad (4)$$

$$k_{\text{nr}} = (1 - \Phi_{\text{fl}}) / {}^1\tau \quad (5)$$

Computational Details All calculations were carried out using density functional theory (DFT) with the CAM-B3LYP functional as implemented in the Gaussian 09 program package and 6-311g (d,p) basis set.[5] The optimization calculations were carried out using the CPCM polarizable continuum model with the dielectric constant of acetonitrile.[6] A vibrational frequency analysis coupling with the CPCM model was carried out in order to confirm the minimum-energy geometry in solution, followed by Time-dependent Density Functional Theory (TD-DFT).[7] TD-DFT calculations included the keyword cis(d) to account for configurational interactions.

Optical photoacoustic z-scan (OPAZ) experimental details For OPAZ-scan measurements a 2.0 mm path length quartz cell was placed at a 45° angle with respect to the incident laser beam (effective path length = 2.83 mm). A custom made sample cell housing unit was used wherein the quartz cell is placed and is filled with water for acoustic signal transmission. Samples were dissolved in spectroscopic grade acetonitrile having a linear absorption coefficient (α) of 345 m⁻¹ at the laser excitation wavelength 688 nm (optical density = 0.3). The output of an optical parametric oscillator (OPO, Continuum Surelite OPO Plus680 - 980 nm, pulse width ~3 ns) was focused onto the sample using a 20 cm focal length lens. The sample was mounted on an automated translation stage (Thorlabs NRT 150) and moved horizontally along the z direction through the focal point of the beam. Each z-scan experiment took roughly 7 minutes in total. Samples were translated along the z-axis over 15 cm in steps of 5 mm. At each position the photoacoustic and optical signals were recorded by averaging the response of 20 laser pulses (@ 10 Hz = 2 sec duration). UV-Vis absorption spectra were recorded before and after each z-scan experiment to ensure the stability of the sample. No degradation was observed under these experimental conditions for the series of dyes presented. Each experiment was repeated 3 times with freshly prepared sample to check for reproducibility. The beam waist (x_0) at focal plane was estimated to be 75 ± 5 μm. The energy incident on the sample was controlled by the combination of a half-wave plate and a linear polarizer. The incident laser energy before the focusing lens was 66 μJ. At the focal point the sample experiences optimum pump intensity, which

decreases gradually on either side of the focus as the sample is translated along the z axis. As the fluence of incident light changes, the optical transmittance varies according to the sample's nonlinear electronic absorption properties. The PA emission was collected using a 10 MHz, 1 inch focal length water immersion ultrasonic transducer (Olympus NDT U8517074).

Photoacoustic tomography For PAT measurements the output of an OPO laser is directed on the sample at a 45° angle using a prism . The sample is placed in a cell housing unit which is filled with water for acoustic signal coupling. A 10 MHz water immersion focused transducer (Olympus V311-SU is placed directly above the sample. The sample is mounted on an automated XYZ translation stage (Thorlabs NRT 100) and moved along the x and y directions in discrete steps to perform 2D raster scan. The PA signal is collected by the transducer and then amplified using a pulse amplifier which was fed to a Lecroy Wavepro oscilloscope for display and data collection. The scanning and data collections are controlled by a Labview routine. By collecting data points along the xy plane, a maximum intensity projection (MIP) is obtained by taking the absolute value of the Hilbert transform of the acquired signal via MATLAB. The MIP image is the map of optical absorption of the sample. The dyes were injected into 1 mm borosilicate capillary tubes and then placed parallel in the Y direction in the bottom of the cell housing unit.

Table SI-1. Absorption and emission data of **1**, **2**, **3** and Cy5 recorded in acetonitrile including fluorescence lifetimes (τ_{fl}), radiative (k_r) and non-radiative (k_{nr}) rate constants.

Compound	λ_{abs} (nm)	$\epsilon \times 10^4$ ($M^{-1} cm^{-1}$)	Φ_{Fl}	λ_{em} (nm)	τ_{fl} (ns)	$k_r, 10^8 (s^{-1})$	$k_{nr}, 10^8 (s^{-1})$	Stokes (cm^{-1})	Shift
1	498	9.44	0.05	588	1.80	0.26	5.29	3074	
2	596	13.85	0.22	705	0.74	2.98	10.55	2595	
3	675	8.35	0.03	736	0.90	0.33	10.78	598	
Cy5	707	10.41	0.01	740	0.03	3.33	330.00	671	

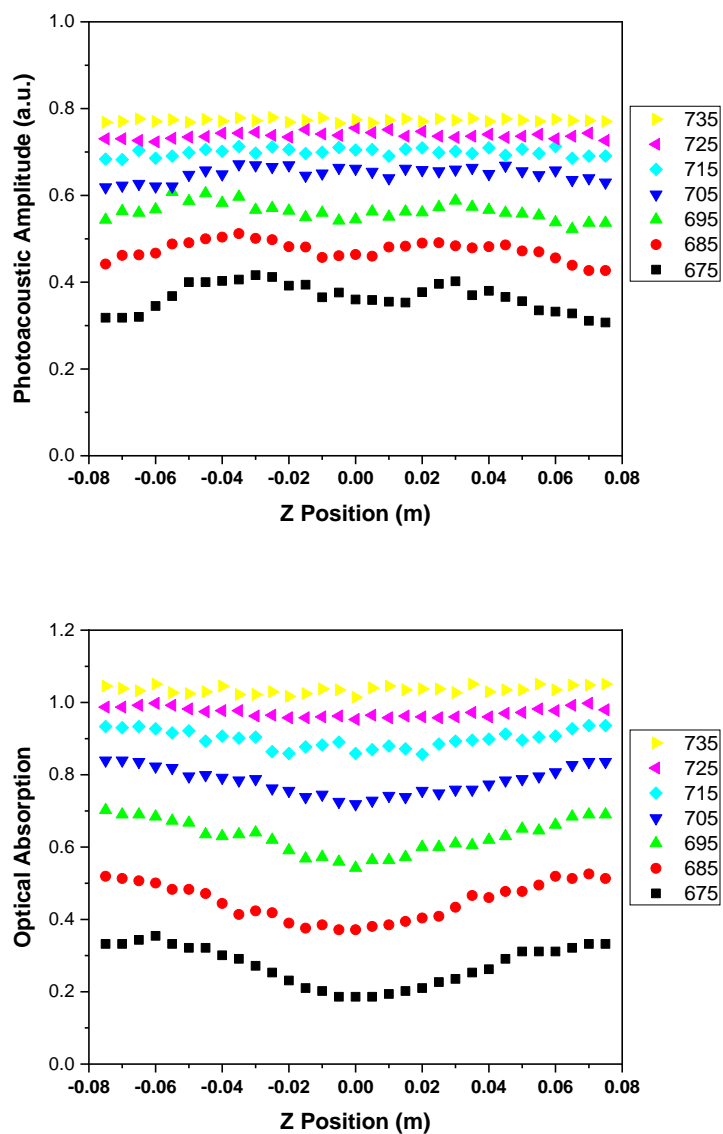


Figure SI-1. Photoacoustic emission (top) and optical absorption (bottom) of dye **3** recorded from 675 – 735 nm excitation.

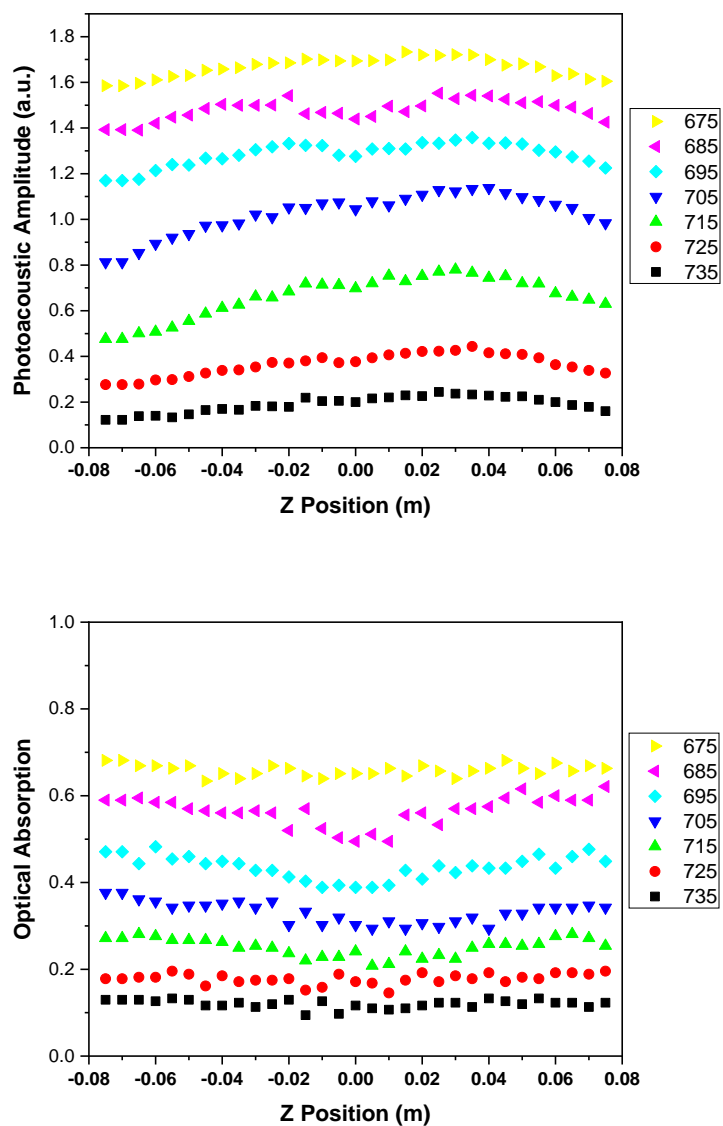


Figure SI-2. Photoacoustic emission (top) and optical absorption (bottom) of dicarbocyanine dye Cy5 recorded from 675 – 735 nm excitation.

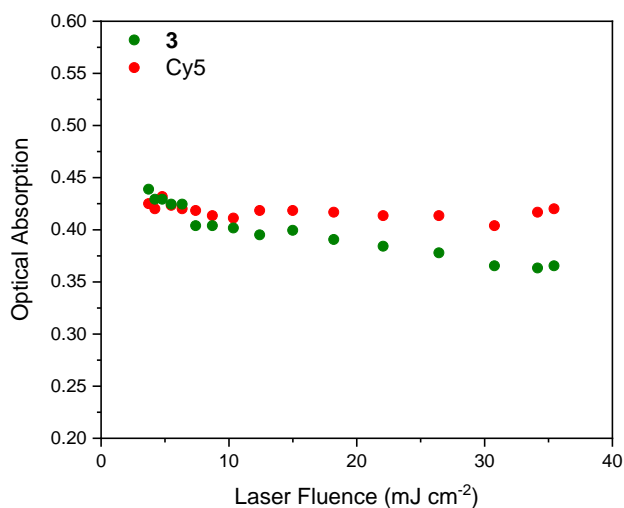


Figure SI-3. Optical absorption of **3** compared to that of the dicarbocyanine dye Cy5 recorded at 688 nm excitation from 5 – 35 J cm⁻² laser fluence.

Table SI-2. Input Z-matrix coordinates for TDDFT analysis of **1**.

CurcuminBF2 (**1**) CAM-B3LYP 6311g dp ACN cis(d) TDDFT

 Charge = 0 Multiplicity = 1

Symbolic Z-Matrix:

C	0.03629	-1.31771	1.20461
C	0.25695	-0.67462	-0.00798
C	-0.0555	-1.32473	-1.19643
O	-0.479	-2.55562	-1.19596
C	0.23781	-0.63642	2.4616
C	0.05079	-0.6504	-2.46866
C	-0.2393	-1.26469	-3.62795
C	0.03233	-1.24485	3.64192
C	-0.17348	-0.69819	-4.96345
C	-0.0586	0.29929	-7.58202
C	0.19702	0.63182	-5.21171
C	-0.49615	-1.50586	-6.05571
C	-0.44072	-1.01517	-7.34917
C	0.25798	1.13119	-6.49299
C	0.19216	-0.67261	4.96689
C	0.47799	0.33807	7.56741
C	0.58403	0.65681	5.18373
C	-0.06081	-1.47384	6.082
C	0.0792	-0.9767	7.36645
C	0.72939	1.16241	6.45582
O	-0.38575	-2.54858	1.24314

B	-0.46868	-3.3962	0.02746
F	-1.64149	-4.12033	0.07443
F	0.64043	-4.22625	-0.01249
H	-0.55801	-2.30093	-3.57312
H	0.37969	0.37983	-2.43015
H	0.60467	0.34636	-0.0244
H	0.56303	0.39354	2.39398
H	-0.29037	-2.28092	3.6147
H	-0.36813	-2.50304	5.94129
H	-0.11302	-1.61241	8.22336
H	0.79345	1.32601	4.35892
H	-0.7901	-2.53531	-5.89014
H	-0.68594	-1.65567	-8.18889
H	0.45571	1.30646	-4.40554
O	0.04048	0.83537	-8.81741
O	0.677	2.41619	-6.69819
O	0.65423	0.88086	8.79126
O	1.16784	2.446	6.62683
H	-0.20426	0.18299	-9.48319
H	0.44002	0.23618	9.47493
C	-0.3381	3.32454	-7.13417
C	0.18721	3.36388	7.11805
H	-0.74673	3.0219	-8.09905
H	-1.13961	3.38569	-6.39309
H	0.14142	4.29646	-7.22965
H	0.67822	4.33287	7.1786
H	-0.65727	3.4268	6.42648
H	-0.1643	3.06952	8.10766

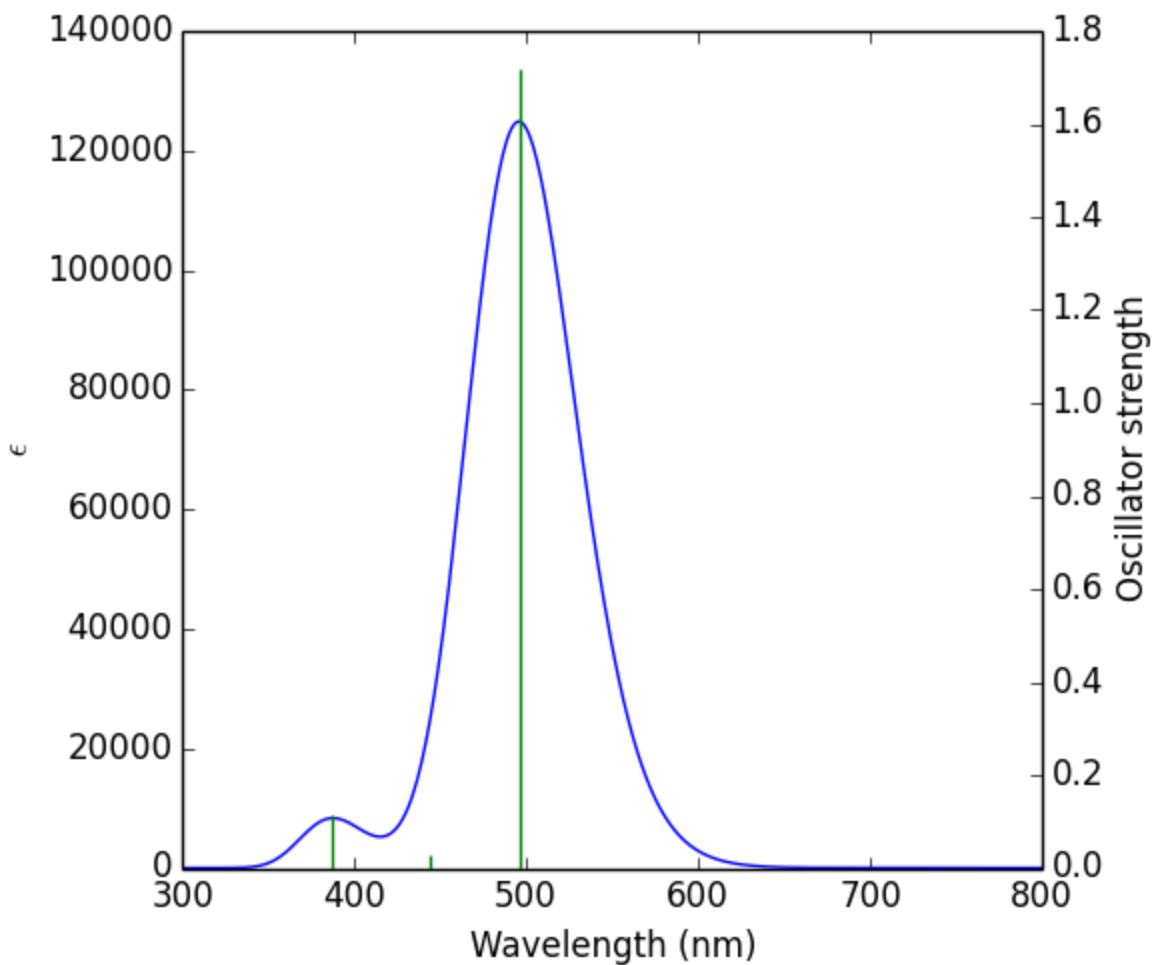


Figure SI-4. TDDFT calculated electronic absorption spectrum for **1**.

Table SI-3. Input Z-matrix coordinates for TDDFT analysis of **2**.

DMAP2CurcuminBF2 (**2**) CAM-B3LYP 6311g dp ACN cis(d) TDDFT

 Charge = 0 Multiplicity = 1

Symbolic Z-Matrix:

C	0.40312	-1.46608	1.19214
C	0.42186	-0.7777	-0.01661
C	0.30336	-1.47586	-1.21409
O	0.25359	-2.78174	-1.22238
C	0.40359	-0.77333	2.45188
C	0.20311	-0.79228	-2.47475
C	0.10229	-1.45728	-3.64484
C	0.39484	-1.43072	3.63057
C	-0.00503	-0.903	-4.97158

C	-0.20863	0.08121	-7.63413
C	-0.04179	0.475	-5.24199
C	-0.07598	-1.76845	-6.07265
C	-0.17404	-1.3054	-7.36529
C	-0.14001	0.95885	-6.52387
C	0.38994	-0.86888	4.95845
C	0.38376	0.12921	7.62366
C	0.3829	0.51062	5.22365
C	0.39243	-1.72859	6.06631
C	0.38955	-1.25885	7.36021
C	0.37996	1.00115	6.50678
O	0.35735	-2.77188	1.21449
B	0.5404	-3.58296	-0.01058
F	-0.33698	-4.6499	0.03159
F	1.85859	-4.02013	-0.06519
H	0.10399	-2.54194	-3.5895
H	0.21646	0.28899	-2.42896
H	0.45843	0.30063	-0.02289
H	0.41132	0.30762	2.39783
H	0.3919	-2.51571	3.58177
H	0.39698	-2.80022	5.899
H	0.39171	-1.96828	8.17439
H	0.37872	1.2192	4.40409
H	-0.05155	-2.83913	-5.90105
H	-0.2244	-2.01908	-8.1742
H	0.00645	1.1877	-4.42743
H	-0.16437	2.02774	-6.67656
H	0.37402	2.0709	6.65527
N	-0.30433	0.55626	-8.90471
N	0.38146	0.61081	8.89536
C	0.3737	2.04236	9.14003
H	-0.51666	2.51989	8.71981
H	0.37534	2.21792	10.21226
H	1.25669	2.52967	8.71575
C	0.38205	-0.30379	10.02327
H	1.26992	-0.94343	10.0237
H	0.38004	0.27065	10.94549
H	-0.50318	-0.94716	10.02195
C	-0.33648	1.98655	-9.15504
H	-0.42073	2.15652	-10.22486
H	-1.19298	2.46263	-8.66842
H	0.57514	2.47959	-8.80386
C	-0.36389	-0.36381	-10.02655
H	-0.43176	0.20595	-10.94918
H	0.53005	-0.99268	-10.0807
H	-1.23915	-1.01778	-9.96643

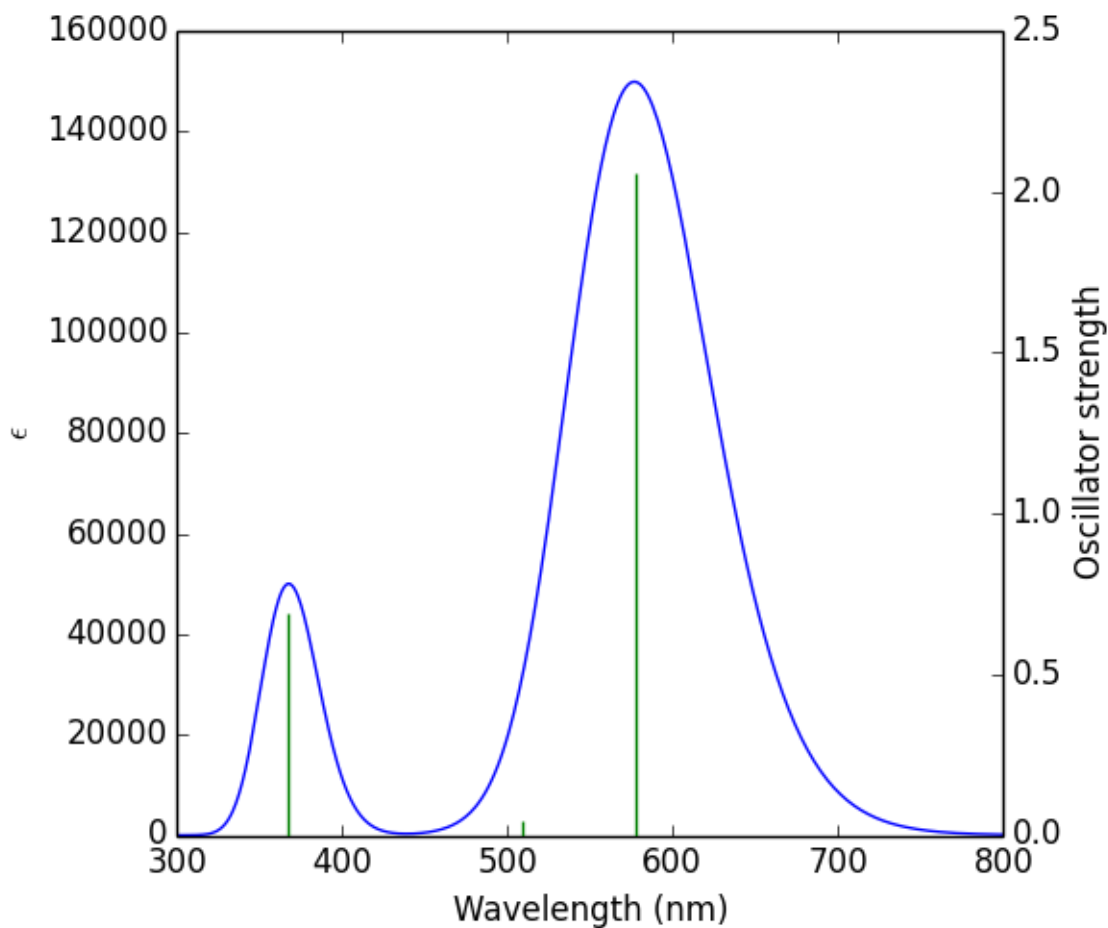


Figure SI-5. TDDFT calculated electronic absorption spectrum for **2**.

Table SI-4. Input Z-matrix coordinates for TDDFT analysis of **3**.

Me2NThCurcuminBF2 (**3**) CAM-B3LYP 6311g dp ACN cis(d) TDDFT

 Charge = 0 Multiplicity = 1

Symbolic Z-Matrix:

C	0.14414	-2.00304	1.22636
C	0.01373	-1.31654	0.0228
C	0.05398	-2.0095	-1.18342
O	0.14682	-3.31723	-1.19769
C	0.20792	-1.31797	2.4806
C	0.02231	-1.33176	-2.44287
C	0.04425	-2.00125	-3.62299
C	0.31754	-1.98068	3.65964
C	0.0194	-1.45979	-4.92918

C	-0.03627	-0.02637	-6.99262
C	0.0364	-2.16928	-6.11155
C	-0.00223	-1.38912	-7.27018
C	0.39317	-1.43196	4.96084
C	0.50042	0.01282	7.01422
C	0.49358	-2.13521	6.14283
C	0.54609	-1.34863	7.29655
O	0.23701	-3.3107	1.24107
B	0.00916	-4.12772	0.03062
F	-1.27839	-4.65498	0.07952
F	0.95288	-5.1411	-0.00162
H	0.08423	-3.08563	-3.58025
H	-0.02072	-0.24998	-2.40685
H	-0.06017	-0.23994	0.02306
H	0.16356	-0.23637	2.44117
H	0.35124	-3.0654	3.62035
H	0.52377	-3.21738	6.15775
H	0.61197	-1.74656	8.29674
H	0.07271	-3.2513	-6.12294
H	-0.00811	-1.79247	-8.27032
N	-0.04945	0.99581	-7.86873
N	0.557	1.03967	7.88307
C	0.30294	2.39898	7.43889
H	-0.75912	2.57234	7.23266
H	0.62735	3.09139	8.21215
H	0.87553	2.61546	6.53522
C	0.51832	0.74594	9.30676
H	1.29683	0.0275	9.56739
H	0.70318	1.66336	9.85992
H	-0.45165	0.3385	9.61112
C	-0.28579	2.35537	-7.41557
H	-0.01875	3.04623	-8.21181
H	-1.33355	2.52084	-7.1411
H	0.34277	2.58148	-6.55242
C	-0.18368	0.69383	-9.28482
H	-0.03614	1.60792	-9.85457
H	0.57569	-0.02642	-9.59248
H	-1.17182	0.28509	-9.52159
S	-0.04889	0.26556	-5.26905
S	0.36198	0.2956	5.29471

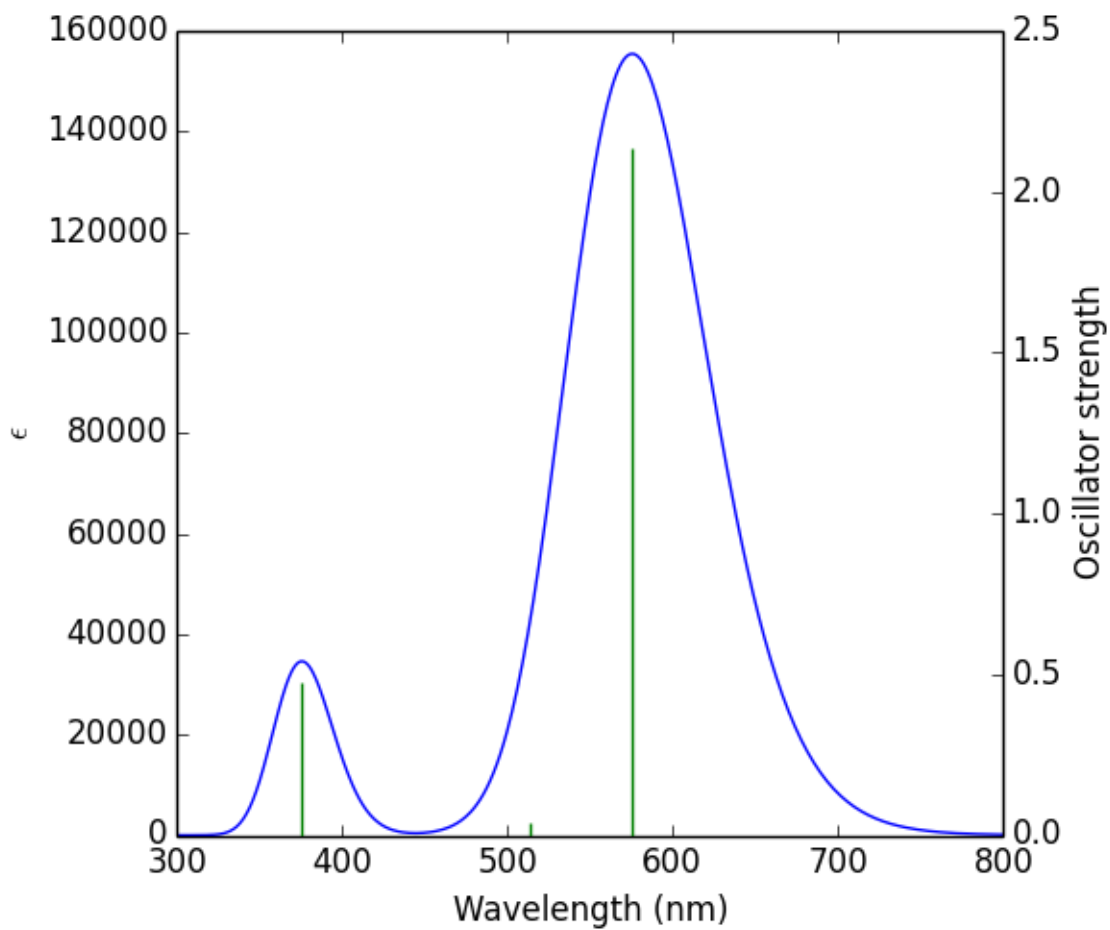


Figure SI-6. TDDFT calculated electronic absorption spectrum for **3**.

References

- [1] K. Liu, J. Chen, J. Chojnacki, S. Zhang, *Tetrahedron Lett.* 54 (2013) 2070-2073.
- [2] G. Bai, C. Yu, C. Cheng, E. Hao, Y. Wei, X. Mu, L. Jiao, *Org. Biomol. Chem.* 12 (2014) 1618-1626.
- [3] X. Zhang, Y. Tian, Z. Li, X. Tian, H. Sun, H. Liu, A. Moore, C. Ran, *J. Am. Chem. Soc.* 135 (2013) 16397-16409.

[4] G.R. Fulmer, A.J.M. Miller, N.H. Sherden, H.E. Gottlieb, A. Nudelman, B.M. Stoltz, J.E. Bercaw, K.I. Goldberg, *Organometallics* 29 (2010) 2176-2179.

[5] Gaussian 09, Revision B.01, M. J. Frisch, G. W. Trucks, H. B. Schlegel, G. E. Scuseria, M. A. Robb, J. R. Cheeseman, G. Scalmani, V. Barone, B. Mennucci, G. A. Petersson, H. Nakatsuji, M. Caricato, X. Li, H. P. Hratchian, A. F. Izmaylov, J. Bloino, G. Zheng, J. L. Sonnenberg, M. Hada, M. Ehara, K. Toyota, R. Fukuda, J. Hasegawa, M. Ishida, T. Nakajima, Y. Honda, O. Kitao, H. Nakai, T. Vreven, J. A. Montgomery, Jr., J. E. Peralta, F. Ogliaro, M. Bearpark, J. J. Heyd, E. Brothers, K. N. Kudin, V. N. Staroverov, T. Keith, R. Kobayashi, J. Normand, K. Raghavachari, A. Rendell, J. C. Burant, S. S. Iyengar, J. Tomasi, M. Cossi, N. Rega, J. M. Millam, M. Klene, J. E. Knox, J. B. Cross, V. Bakken, C. Adamo, J. Jaramillo, R. Gomperts, R. E. Stratmann, O. Yazyev, A. J. Austin, R. Cammi, C. Pomelli, J. W. Ochterski, R. L. Martin, K. Morokuma, V. G. Zakrzewski, G. A. Voth, P. Salvador, J. J. Dannenberg, S. Dapprich, A. D. Daniels, O. Farkas, J. B. Foresman, J. V. Ortiz, J. Cioslowski, and D. J. Fox, Gaussian, Inc., Wallingford CT, 2010.

[6] J. Tomasi, B. Mennucci, R. Cammi, *Chem. Rev.* 105 (2005) 2999-3093.

[7] G. Scalmani, M.J. Frisch, B. Mennucci, J. Tomasi, R. Cammi, V. Barone, *J. Chem. Phys.* 124 (2006) 94107.